The use and limitations of modern technologies for slow, vegetated landslide monitoring – Chin Coulee Landslide

Evan Deane, Renato Macciotta, Michael Hendry
University of Alberta, Edmonton, AB, Canada
Chris Gräpel
Klohn Crippen Berger, Edmonton, AB, Canada
Roger Skirrow
Alberta Transportation, Edmonton, AB, Canada

ABSTRACT
Geohazard monitoring for networks of linear infrastructure have traditionally involved time-intensive and intrusive monitoring methods using permanently installed instruments. These traditional methods often require expensive mobilization and site access for larger vehicles compared to more modern methods. Combining traditional instrumentation and modern monitoring technologies allows for greater understanding of hazards and development of risk reduction strategies. These technologies provide an economically efficient means of improving monitoring processes, often minimizing the need for costly permanent instrumentation installation.

This paper presents the application of light detection and ranging (LiDAR) and differential global positioning systems (GPS) to improve upon sparse historical records and enhance the understanding of the development, progression, and mechanisms of landslides. A number of issues involving their use in slow-moving, vegetated landslides is also discussed. As a case study, we use a slow-moving vegetated landslide located in Southern Alberta called the Chin Coulee landslide.

RÉSUMÉ
La surveillance des géorisques pour les réseaux d'infrastructures linéaires a toujours fait appel à des méthodes de surveillance chronophages utilisant des instruments installés en permanence. Ces méthodes traditionnelles nécessitent souvent une mobilisation et accès au site coûteux pour les véhicules plus gros par rapport aux méthodes plus modernes. La combinaison de l'instrumentation traditionnelle et des technologies de surveillance permet de mieux comprendre les dangers et d'élaborer des stratégies de réduction des risques. Ces technologies constituent un moyen économiquement efficace d'améliorer les processus de surveillance, minimisant souvent le besoin d'une installation coûteuse en instrumentation.

Cet article présente l'application du système de détection et de télémétrie par la lumière et du système de positionnement global différentiel afin d'améliorer les archives historiques éparses et de mieux comprendre le développement, la progression et les mécanismes des glissements de terrain. Un certain nombre de problèmes liés à leur utilisation dans les glissements de terrain végétalisés à déplacement lent sont également abordés. Comme étude de cas, nous utilisons un glissement de terrain végétalisé à déplacement lent situé dans le sud de l'Alberta appelé glissement de terrain Chin Coulee.

1 INTRODUCTION

Geohazards have a large impact on infrastructure, with estimated damages due to landslides in Canada reaching $200 – 400 million annually (NRC, 2008). These costs are likely to increase as infrastructure ages, population density increases, and environmental triggers become more intense and frequent. Service interruptions due to damaged powerlines, roads, railways, or pipelines pose economic, social and environmental impacts. Geohazard instrumentation monitoring programs are important as part of a robust risk management plan.

As monitoring systems continue to develop, improve, and evolve, new monitoring methods integrated with traditional instrumentation can provide insights that are unattainable from traditional instrumentation. These new methods often involve non-intrusive, non-permanent installations which allow for reuse on multiple sites.

The combined use of historical instrument data and modern technologies is becoming commonplace. Many new monitoring methods are data intensive, so before the geotechnical community can adopt the use of these modern technologies, the quality of the collected data, as well as an understanding of the limitations that these technologies face is required. This is especially important in difficult ground conditions such as remotely located, slow-moving, vegetated, deep-seated, large scale landslides.

This paper illustrates a case study in which historical slope indicator and piezometer instrumentation information is improved by modern monitoring methods, including terrestrial laser scanning (TLS) LiDAR change detection, and differential GPS systems. An analysis of the limitations that were faced during the application of these technologies is made, and the current state of whether they are viable options for monitoring is analyzed. The Chin Coulee landslide meets all of the above described criteria for difficult ground conditions.

2 THE CHIN COULEE LANDSLIDE

The Chin Coulee landslide is situated on the northern slope of the Chin Coulee reservoir, adjacent to Alberta Highway 36 (Figure 1). Highway 36 is a rural two-lane paved highway with average annual daily traffic of 880 vehicles (Government of Alberta, 2017). The highway provides a north-south connection over the Lower Chin Coulee reservoir. An elevated causeway provides access across the reservoir and presents a major constraint on realignment options at the landslide site. Headscarp retrogression threatens Highway 36, and loss of the roadway at this location would result in a detour length of about 25 km to the nearest crossing of Chin Coulee. Chin Coulee valley is about 55 m deep, 1300 m wide at prairie level, and 550 m wide at reservoir level. Natural valley slope inclinations vary but are generally about 6H:1V (9^{o}).

Figure 1. Location of Chin Coulee Landslide in Alberta (base imagery from ESRI, 2019)

A significant local realignment of the highway was performed in 2016 and if further highway damage occurs, a major regional realignment would be required. This major realignment proposes shifting the road more than 50 m, outside the landslide zone entirely. Outside of major damage to the highway, this realignment is contingent on reconstruction of the causeway, anticipated in 2030. In the meantime, monitoring of landslide progression will be required; traditional technologies generally do not provide this duration of monitoring and would require periodic costly replacement.

2.1 Geology and Landslide Characteristics

Bedrock and surficial geology maps (Fenton et al., 2013 & Prior et al., 2013) indicate that Chin Coulee valley is a glacial meltwater channel incised though a thick layer of stagnant ice moraine (till materials) and into Foremost Formation bedrock. The Foremost Formation is a unit within the Belly River Group stratigraphic unit of the late Cretaceous Western Canadian Sedimentary Basin. This bedrock unit is made up of discontinuous layers of mudstones, clayey siltstones, silty shales, and sandstones.

Site specific stratigraphy information was derived from investigation and instrumentation programs undertaken over many years. Standpipe piezometer and slope inclinometers were installed by Golder and Associates in 1998 (GA98-1 – 5) (Golder and Associates, 1998). Slope inclinometers and piezometers were installed by AMEC in 2002 and subsequently destroyed during a road and ditch realignment in 2012 (AMEC, 2013). Another slope inclinometer was installed by AMEC Foster Wheeler in 2015 (AMEC FW, 2015). Klohn Crippen Berger (KCB) installed two slope inclinometers between the highway and the head scarp in early 2018 to monitor for slide retrogression (KCB, 2018).

Medium plasticity clay fill material from the initial highway construction and subsequent realignments and regrading is exposed at the headscarp.

Below the fill, and mantling the valley slope, is a silty clay till with traces of fine gravel. The till has low to medium plasticity and is very stiff to hard. Thickness of the till varies from roughly 20 m at the toe of the slope to 35 m near the headscarp.

A layer of highly fractured shales and coal was encountered at a depth of 32 m and 17 m in boreholes GA98-4 and GA98-5 respectively (see Figure 2 and Figure 3). It is believed that the Chin Coulee landslide is a translational retrogressive landslide seated within this highly fractured bedrock zone. The slide is about 350 m wide and up to 45 m deep. The length of the slide is approximately 200 m long with the toe of slide within the reservoir. The total slide volume is estimated at approximately 2 million cubic meters, based on measurement along the proposed failure plane and current landslide extents.

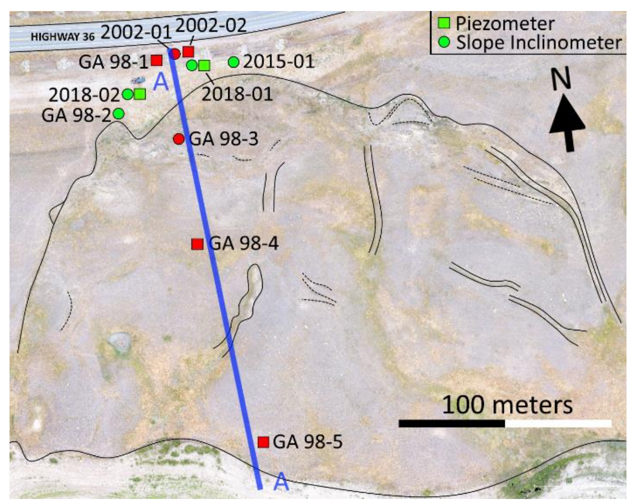

Figure 2. Instrument Locations on Chin Coulee (Green symbols indicate currently functional instruments)

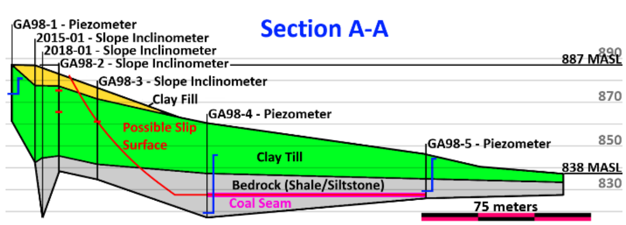

Figure 3. Chin Coulee Stratigraphy (Typical cross section)

2.2 Material Properties

Borehole samples taken in 2015 were tested for moisture content, Atterberg limits, grain size distribution, direct shear (DS), and consolidated undrained (CU) triaxial tests. Testing focused on the clay fill and clay till material. Laboratory results are summarized in Table 1. Samples were not obtained at the slide plane depth.

Table 1. Soil Characteristics of Clay Fill and Clay Till on Chin Coulee (AMEC FW, 2015)

Characteristic	Clay Fill	Clay Till	Clay Till	Clay Till
Depth of Sample (m)	3.2	10.0	14.0	15.2
In-situ Moisture (%)	11 – 19	12.8	10 – 20	10 – 20
Liquid limit (%)	38.7	-	45.7	28.9
Plastic limit (%)	21.7	-	21.6	16.0
Bulk Density (kg/m^3)	2097	2184	-	-
CU Triaxial, Peak Friction Angle (°)	27.5	-	-	-
DS, Peak Friction Angle (°)	-	25.6	-	-
DS, Cohesion (kPa)	-	21.5	-	-

2.3 History of Activity

The history and evolution of the Chin Coulee landslide is well understood through analysis of the multiple reports submitted to Alberta Transportation, as well as historical air photos available through the Alberta Air Photo Library.

Before 1950, Highway 36 was located within the current valley floor (Figure 4). The highway was relocated to the valley wall, above the current landslide location, after impoundment of the Chin Coulee reservoir (Figure 5).

Between 1960 and 1970, Highway 36 was shifted south towards the current landslide headscarp to facilitate improvements to the highway curve alignment. The realignment involved placement of road fill downslope of the highway to build the embankment. This fill extended onto the area of slope instability (Figure 6).

In the fall of 1978, following significant precipitation, the first major movement event on Chin Coulee occurred (AMEC, 2000). Based on photogrammetry models created from post-failure air photos conducted in 1982, vertical displacement along the main scarp was approximately 1 meter (Figure 7). No other significant movement events were noted until 1997, where movement was again noted by Alberta Transportation and the Chin Coulee landslide was added to the Alberta Transportation Geohazard Risk Management Program (GRMP) as site S005 (Southern Region Site 5) (Golder and Associates, 1998).

Since 1997 there has been very little movement recorded by the instrumentation (AMEC FW, 2015). The largest detected period of movement occurred in 2009, with a peak movement rate of 5 mm/year being observed in SI GA98-2 over an 8-month time period from September 2008 to May 2009 (AMEC FW, 2015). It should be noted that no currently functional instruments are located within the sliding mass, only retrogression is truly being measured.

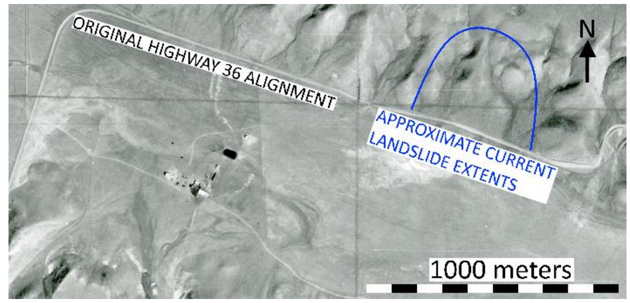

Figure 4. 1945 Air photo of Chin Coulee (Alberta Air photo Library, 1945)

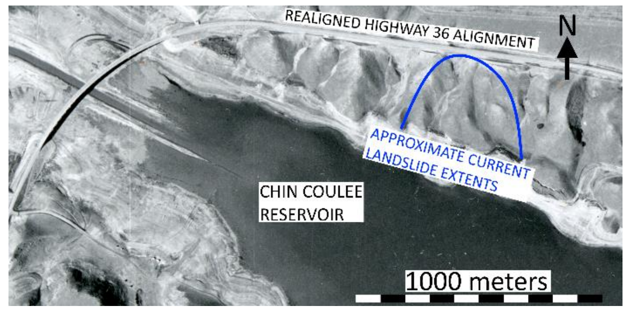

Figure 5. 1960 Air photo of Chin Coulee (Alberta Air photo Library, 1960)

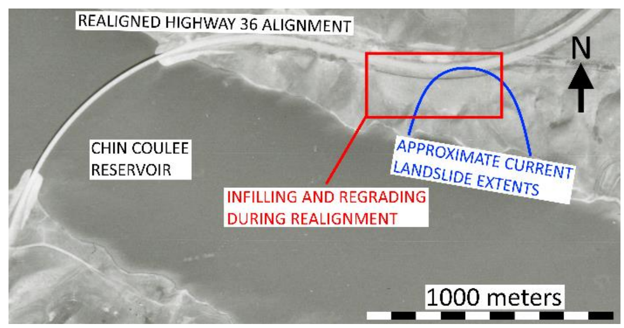

Figure 6. 1970 Air photo of Chin Coulee (Alberta Air photo Library, 1970)

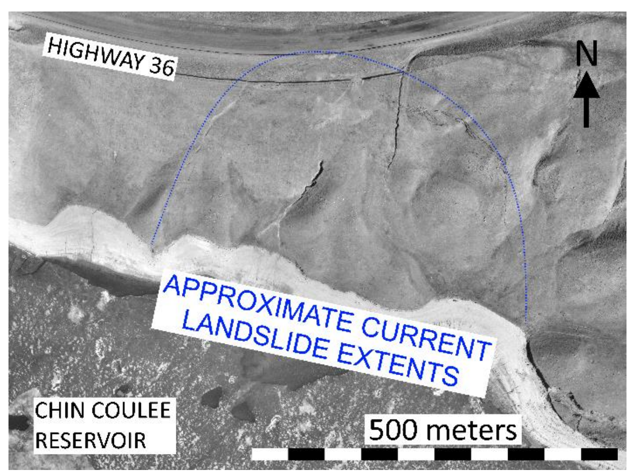

Figure 7. 1982 Air photo of Chin Coulee (Alberta Air photo Library, 1982)

3 APPLICATION OF MODERN MONITORING TECHNOLOGIES

3.1 Differential GPS

Differential GPS systems involve the use of a "fixed-point", which is located in a stable "non-moving" area, as a means of acquiring and correcting for errors present within the system due to atmospheric properties. By correcting these errors, the systems relative position can be vastly improved over traditional GPS measurements (Langley, 1998).

A differential GPS system consisting of ten Geocubes™, an all-in-one differential GPS system, was installed on the Chin Coulee landslide. This system is similar to systems previously installed on the 10-Mile and Ripley slide in British Columbia (Rodriguez et al., 2018) and consists of a coordinator, which acts as a central processing hub for the system, a "fixed point", and nine mobile points strategically placed around the landslide. Figure 8 shows the location of the ten GPS units, as well as the coordinator. The "fixed point" and coordinator are approximately 950 m away from the remaining GPS units.

The differential GPS system was installed as a means of obtaining continuous movement data for targeted regions of the landslide. Continuous acquisition of movement data and monitoring of GPS system health was achieved through the use of a mobile data plan. Due to the remote location this method of data acquisition was preferred, and more economical, than travelling to site to download data at regular intervals.

Figure 8. GPS Unit Location on Chin Coulee (base imagery from ESRI, 2019)

3.1.1 Differential GPS System Installation

The GPS system on Chin Coulee was installed in June of 2018 and continuous recording began on July 11th, 2018, following relocation of the fixed point (see Figure *8*).

Previous differential GPS system installations on 10-Mile slide and Ripley slide employed the use of slotted steel angle for GPS posts, however on Chin Coulee, hand augered deck screw piles were used. Each GPS unit was equipped with a 10-Watt solar panel and two 12-Volt, 100 Ah batteries. This power setup ensured that system power would be available all year round. Figure 9 shows a typical GPS and battery box setup.

Due to the ground conditions on the site, difficulties were experienced during post installation. Frequently the pile would get stuck in gravel and had to be relocated, as a result, embedment depth was limited to 0.8 – 0.9 m. The auger screw also disturbed the soil, reducing post rigidity. This was alleviated by packing rocks into the post base with a sledge hammer after installation.

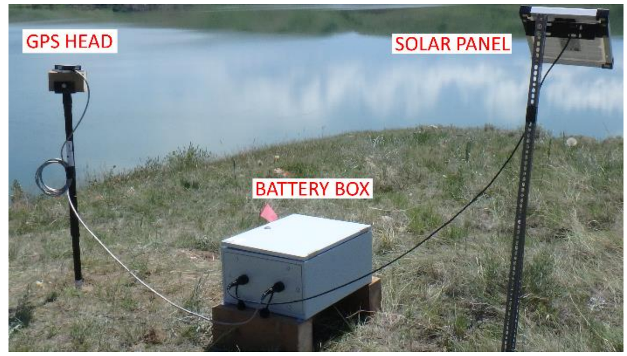

Figure 9. GPS and Battery Box Setup on Chin Coulee

Due to the distance between the coordinator and the GPS units, radio connection required the use of directional antennas on two of the GPS units. It was also found that the GPS units had to be mounted roughly a meter above the ground in order to communicate between each other, a requirement for the system employed. GPS unit 152 near the headscarp (See Figure 8) had to be raised over 2 meters in order to connect, due to its line of site to the rest of the system. This installation height likely leads to an increased amount of error due to movement of the support post for this GPS unit.

3.1.2 Differential GPS System Limitations

GPS systems have an inherent limit in point accuracy due to atmospheric and local effects. For the GPS units used on Chin Coulee, 10-Mile, and Ripley slide, the manufacturer specified precision is typically 1 – 2 mm (Ophelia-sensors, 2018). Based on a 24-hour moving window, standard deviation of Northing and Easting is typically 1 – 2 mm on 10-Mile. On Chin Coulee, a 24-hour moving window has a standard deviation of 2 – 4 mm (black scatter points in Figure 10).

The differential GPS system employed on 10-Mile slide was overall a success and showed meaningful movement trends in several GPS units (Rodriguez et al., 2018). The GPS units on Chin Coulee also showed trends, although not as consistent as that of 10-Mile. This is in part due to the standard deviation of movement present in the Chin Coulee data set. With expected movement levels of 20 – 45 mm each year, daily standard deviations of 2 – 4 mm create measurement errors for short term sampling and impact data trends.

Applying a 2-day moving average to Chin Coulee movement data resulted in large measurement scatter. Predictable movement trend patterns begin to arise once the averaging window increased to 20 days. The high standard deviation of the data reduces the viability of short term, month-to-month data sampling. Movement trends can only be observed by applying larger average windows. These measures were necessary due to the slow movement levels and relatively large standard deviation of the data on Chin Coulee. With faster moving landslides, such large averaging windows may not be necessary to obtain movement trends.

Figure 10 highlights the varying levels of movement and standard deviation of movement in three GPS units on Chin Coulee and 10-Mile. 10-Mile slide data runs from April to November of 2017. Chin Coulee data was taken from a 9-month data set running from July of 2018 to April of 2019, notably a longer data set than LiDAR data comparisons shown in later sections.

Displacement values shown in these plots are not a standard cumulative displacement. Displacement is determined by computing the Euclidian distance from the initial position to the current position. As such, negative movements are possible in the case of movement back towards the initial position.

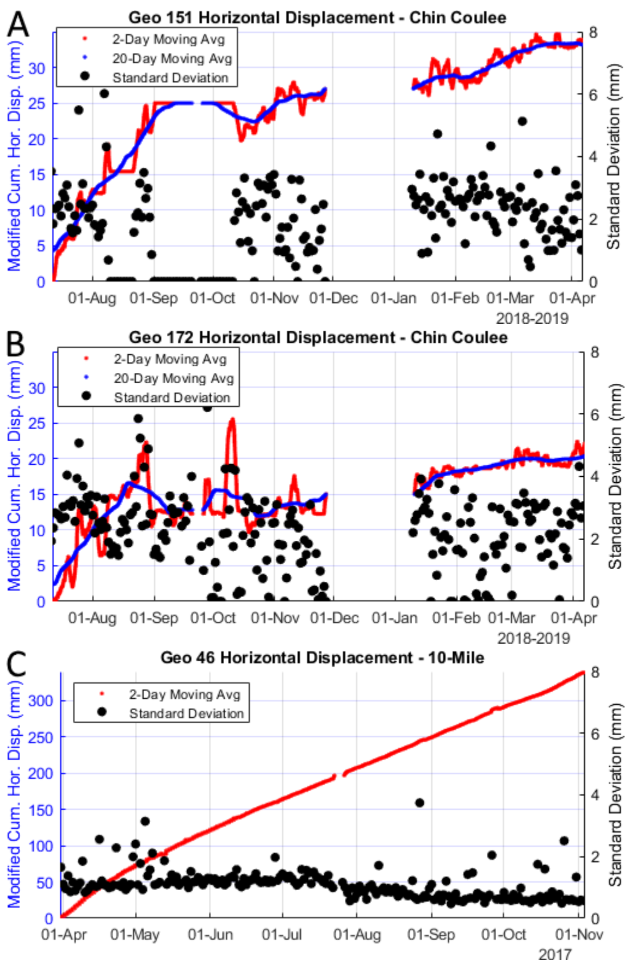

Figure 10. GPS 151 (A) and 172 (B) on Chin Coulee and GPS 46 (C) on 10-Mile

The height of installation for the GPS units may have also played a role in the errors observed on Chin Coulee slide. As the ground moves, the support posts also move. This movement may result in tilting of the post, which exaggerates the movement on the GPS. For example, a post which is 1.2 m tall only needs to tilt 2° in order to correspond to a GPS movement of 42 mm. As the ground movement on Chin Coulee is typically extremely slow, such a movement could cause unwarranted alarm.

Given these limitations, GPS data on Chin Coulee is preliminary and more time might be required to show real displacement trends. Moreover, five of the nine GPS units on site are currently showing movement away from the expected direction, in some cases uphill. Figure 11 outlines the measured cumulative displacement vectors from July 11, 2018 to April 6, 2019, with unexpected movements signified with red and yellow vectors.

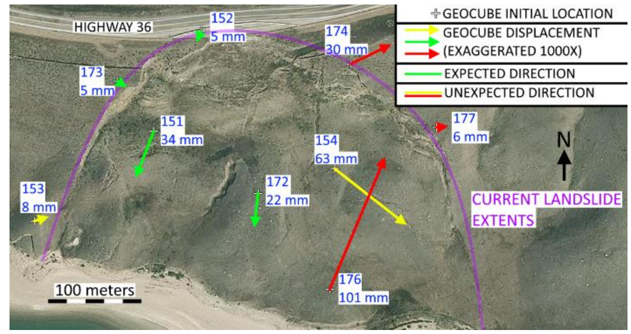

Figure 11. GPS Unit Movements on Chin Coulee from July 11, 2018 to April 6, 2019 (base imagery from ESRI, 2019)

The unrealistic displacement orientations shown in Figure 11 appear to mostly be due to sudden and large movement events shown in GPS data. It is believed that these jumps are not associated with sudden movement of the landslide mass, due to the displacement directions, as well as associated vandalism that occurred during similar time periods.

These events impact the expected magnitude of yearly displacement for Chin Coulee, and lead to inaccuracies in displacement direction. Figure 12 and Figure 13 show such jumps on GPS units 154 and 174 on Chin Coulee. Similar jumps were present on GPS units 153 and 176.

It is believed that these movements are due to vandalism to the system and it was decided that these movements should be removed to see the underlying movement trends of the GPS units.

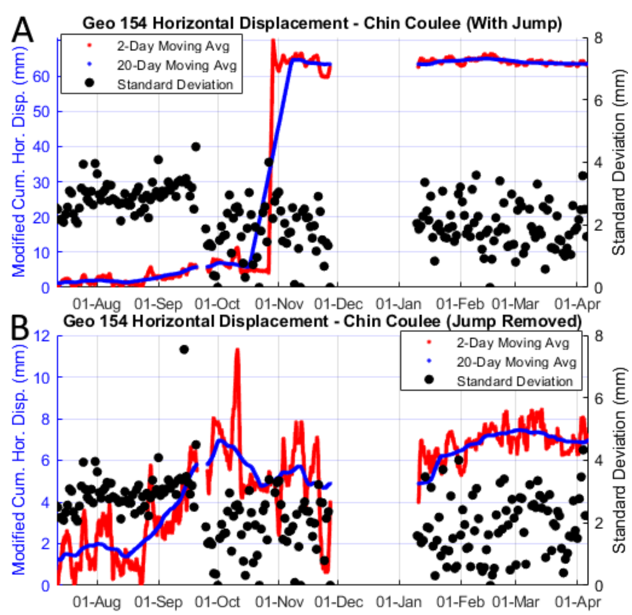

Figure 12. GPS Unit 154 on Chin Coulee (A) With Jumps (B) Jumps Removed

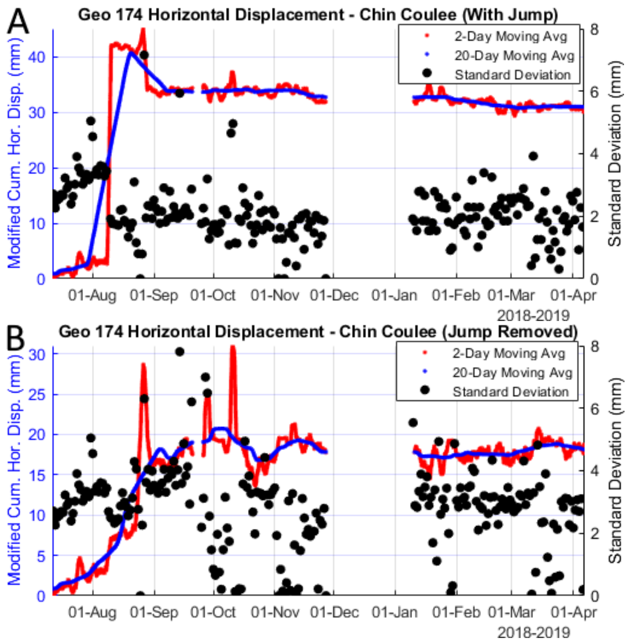

Figure 13. GPS Unit 174 on Chin Coulee (A) With Jumps (B) Jumps Removed

Removal of these jumps was completed by removing data from the beginning of the sudden movement until the end of the sudden movement and fitting the remaining data to the same value. Displacement vectors associated with the corrected GPS movement data is shown in Figure 14. Removal of these jumps leads to a much more consistent amount of movement throughout the slide and eliminates movement in unexpected directions from all but GPS unit 177, which did not contain any jumps in the data set.

GPS movement was recorded over a 269-day period from July 11, 2018 to April 6, 2019. Correspondingly, yearly movement rates for Chin Coulee ranges from 20 – 40 mm/year, based on movement rates after jump removal.

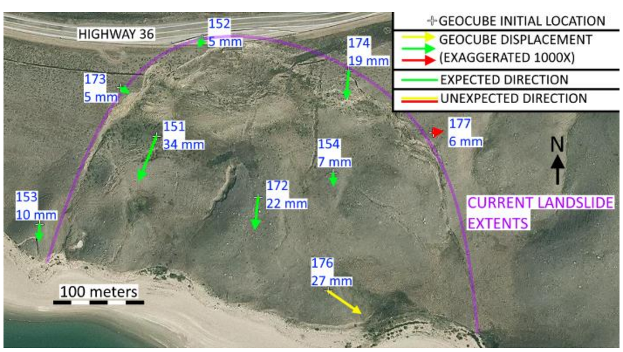

Figure 14. GPS Unit Movements on Chin Coulee from July 11, 2018 to April 6, 2019 (Jumps Removed) (base imagery from ESRI, 2019)

3.2 Terrestrial Laser Scanning LiDAR

LiDAR was employed on Chin Coulee as the primary means of achieving complete spatial monitoring coverage. The first LiDAR scan was performed on July 10, 2018 however, this scan was only taken from two locations and significant portions of scan extents were hidden due to the line of sight of the scanner. Subsequent scans used three separate locations. Figure 15 shows the location of the three LiDAR scan locations relative to the landslide.

LiDAR scanning was completed using an Optech ILRIS-LR laser scanner. This scanner features a laser wavelength of 1064 nm, a pulse frequency of 10 kHz, and a beam divergence of 0.014324° (Teledyne Optech, 2019). Average scan distance on Chin Coulee was roughly 950 m.

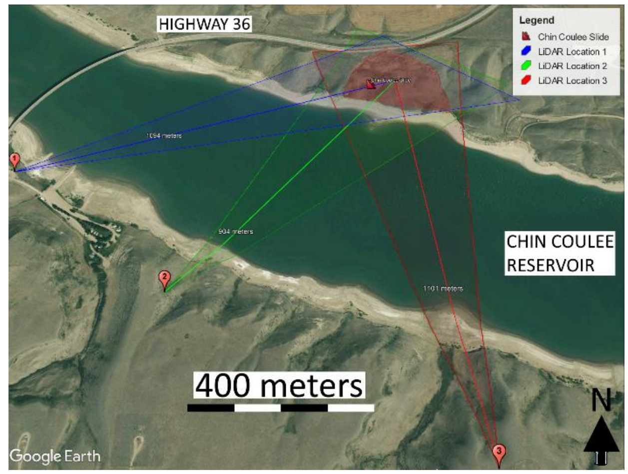

Figure 15. LiDAR Scan Locations on Chin Coulee (Google Earth, 2015)

3.2.1 LiDAR Change Detection and Level of Detection

LiDAR change detection was performed using the Multiscale Model to Model Cloud Comparison (M3C2) algorithm. M3C2 operates by averaging the distance between points on adjacent point clouds that fall within a user-defined size of cylinder, positioned normal to the surface of one point cloud. M3C2 was selected due to its superior performance for distance calculations in natural environments by accounting for uncertainty regarding surface roughness and registration (Lague et al., 2013).

Change detection was performed between the first and second scans, captured on July 10, 2018 and August 23, 2018. Point cloud analysis was conducted with CloudCompare^{TM} point cloud software (CloudCompare, 2019). Using an iterative closest point matching algorithm, a root mean square (RMS) error of 90 – 100 mm was achieved for matching between scans.

The level of detection (LOD), calculated as the 95th percentile of movement in the "non-moving" flanks of the landslide, was 80 mm. Removal of all points within this detection limit removed 87% of points within the active landslide region, with the remaining points visually evenly dispersed throughout the scan (see Figure 16). This indicates that most movement within the landslide is less than 80 mm and is below the detectible limit. Based on expected movement from GPS data, movement during this scanning period would have been at most 4.7 mm, below the LOD. Areas in Figure 16 indicating movement near the headscarp and the right toe of slope, are quite vegetated with tall prairie grasses and dense shrubs that likely had an impact on change detection results in these regions.

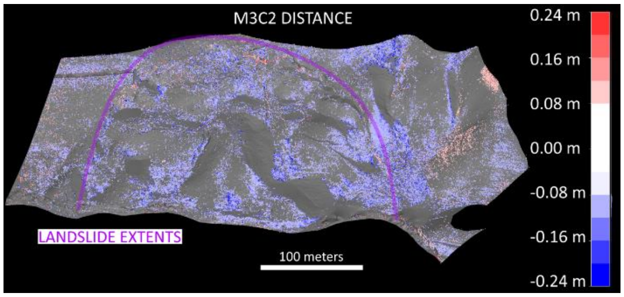

Figure 16. M3C2 Results Between July 10 and August 23, 2018 on Chin Coulee (CloudCompare, 2019)

3.2.2 LiDAR Change Detection Limitations

Two significant limitations were identified during LiDAR scanning on Chin Coulee. The first, and most meaningful is LOD limitations. If landslide movement between scans is below the LOD, movement will not be detectable during that time step. This means that monitoring campaign duration must account for expected levels of movement. Abellan et al. (2009) suggests that movement must exceed two times the standard deviation of movement detected in a non-moving area to be identifiable as real movement. In the case of Chin Coulee, for the July 10 – August 23, 2018 scan this corresponds to movement exceeding 98 mm. It is likely that this requirement can be lowered through better scanning conditions, and that a time span between scans of 6 months would be adequate for observing movement.

Achievable LOD is based on both site-specific characteristics, as well as equipment (Lague et al., 2013). Sites with significantly more vegetative cover will have worse levels of detection due to poor point cloud registration and bare earth model generation. Measures can be taken to improve scanning on vegetated sites, including the use of "last reflection" options available within many LiDAR scanners, as well as vegetation classification tools available within point cloud software. Hardware solutions, such as ground control points, may also improve point cloud registration (Alba et al., 2006).

Wind combined with vegetation appears to also have an impact on point cloud generation. Scans performed during windy weather on Chin Coulee produced point clouds with noticeably more grasses and bushes left unclassifiable. This created problems with point cloud registration, erroneously interpreted ground movement due to vegetation growth, and significantly increased the minimum LOD. The October 13, 2018 scan was impacted by wind gusts exceeding 80 km/h during scanning. Figure 17 shows the resulting change detection, with major striping and vegetation left over, impacting point cloud registration and change detection. Further investigation into the effects of wind conditions would be required to understand the LOD for this scan.

In the case of Chin Coulee, LiDAR generated point clouds were classified using the "Otira_vegetsemi" classifier in CloudCompare, which delivered the best vegetation classification, based on visual inspection (Brodu et al., 2012). Custom CANUPO classifiers were tested as well but delivered similar results. CANUPO classification reduced the remaining vegetation, although did not remove it entirely. Manual removal of the remaining vegetation was deemed unfeasible due to minute size and large extents.

Other methods for bare earth DEM generation include cloth simulation filtering (CSF), outlined by Zhang et al. (2016) and statistical outlier removal (SOR) filtering. CSF and SOR filtering were tested after CANUPO classification. It was seen that neither method significantly improved bare earth DEM generation over CANUPO classification alone.

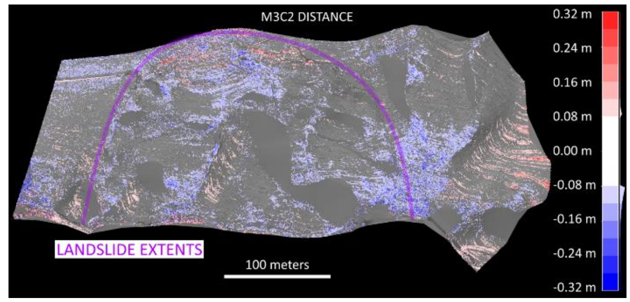

Figure 17. M3C2 Results Between July 10 and October 13, 2018 Showing Wind Impact (CloudCompare, 2019)

The required scanning distance on Chin Coulee is another potential limitation. The average scanner distance was over 950 m from scanner to target due to the reservoir. Long scan distances in combination with rough irregular surfaces, such as those created by vegetation, can lead to measurement uncertainty due to laser enlargement. The scanner used for this research had a positional error perpendicular to the scanner line of site of 80 mm at 1000 m (Teledyne Optech, 2019). The angle of incidence of the scanning surface also has an influence on point positional error, which would further increase this positional inaccuracy (Fey et al., 2017). The average angle of incidence at Chin Coulee is roughly 80º to the scanner.

Vegetation levels in some regions of Chin Coulee make change detection difficult, but with data collected during good scanning conditions, and adequate time between scans, change detection should be possible. Based on movement levels in GPS data ranging from 20 – 40 mm/year, roughly 6 months between scans would be required to begin to see movement above the LOD. Additional scanning is scheduled for May of 2019 and movement levels exceeding 30 mm are expected in some active regions.

4 CONCLUSIONS

Most slope instrumentation on the Chin Coulee landslide focused on monitoring for potential landslide retrogression impacting the highway. In order to capture movement along the sliding plane, instruments must be installed into the bedrock, up to 50 m deep in some areas. This poses a considerable cost for replacement. By applying modern technologies to this site, it was possible to collect information that provides an enhanced understanding of the landslide processes at lower costs than increasing the density of intrusive downhole instrumentation.

By employing a differential GPS system on Chin Coulee, it was possible to increase movement monitoring frequency and accuracy, however the implementation was not as successful as in previous installations on 10-Mile and Ripley slides. When installing differential GPS systems care must be taken in order to minimize system error. The means in which you install the system can lead to erroneous movement, especially when expected slide movement is extremely low. A rigid post system with adequate embedment depth is necessary for obtaining representative ground movements. The expected level of movement also plays an important role in how long monitoring must be conducted prior to obtaining clear displacement trends. In the case of Chin Coulee, movement levels were erratic when looking at short term durations (month to month), but trends began to emerge at 8 or 9-month durations with 20-day moving averages. Care must also be taken to analyze the data obtained from GPS data for accuracy, and steps should be taken to deal with erroneous data associated with any forms of vandalism.

Chin Coulee showcased several issues for the application of LiDAR in slow-moving, vegetated landslides. Vegetation levels made generation of bare earth models difficult, and in some locations, seemingly not possible. Computation of change between subsequent models indicated that movement levels in vegetated regions were inaccurate, due to unclassified vegetation impacting the change detection procedure. Due to the low levels of movement observed on Chin Coulee slide, movement was below the obtainable reliable level of detection. This meant that calculated movement levels were not possible in the time frame between available scans. In the case of Chin Coulee, movement levels range from 20 – 40 mm/year, requiring a duration of roughly 6 months between scans to begin to obtain detectable levels of movement.

Although the application of these technologies on Chin Coulee faced problems due to movement levels and vegetation, it posed a valuable challenge for determining the limits of these technologies in difficult conditions. With additional LiDAR scans and additional GPS data, which will be collected during the Spring and Summer of 2019, it is believed that movement levels will allow for a more conclusive discussion regarding Chin Coulee movement trends and mechanics.

5 ACKNOWLEDGMENTS

This research was made through the Railway Ground Hazard Research Program, funded in part by Natural Sciences and Engineering Research Council of Canada, the Canadian Pacific and Canadian National Railway.

I’d also like to extend a special thank you to Alberta Transportation, Klohn Crippen Berger, Hanh Hong, Jorge Rodriguez, and Hasmik Manandyan, who helped set up the GPS system.

6 REFERENCES

Abellán, A., Jaboyedoff, M., Oppikofer, T., and Vilaplana, J.M. 2009. Detection of Millimetric Deformation Using a Terrestrial Laser Scanner: Experiment and Application to a Rockfall Event, *Natural Hazards and Earth System Science,* 9: 365-372.

Alberta Air photo Library. 1945 Flight Index A7764(6).

Alberta Air photo Library. 1960. Flight Index YC414(52).

Alberta Air photo Library. 1970. Flight Index AS1052(24).

Alberta Air photo Library. 1982. Flight Index 2448(144).

AMEC. 2000. Southern Region Landslide Monitoring – Spring 2000 Assessment Report, *Geotechnical Risk Management Plan*.

AMEC. 2013. Instrumentation Monitoring Results – December 2013 Report, *Geotechnical Risk Management Plan*.

AMEC FW. 2015. Instrumentation Monitoring Results – December 2015 Report, *Geotechnical Risk Management Plan*.

Alba, M., Fregonese, L., Prandi F., Scaioni, M., and Valgoi, P. 2006. Structural Monitoring of a Large Dam by Terrestrial Laser Scanning, *Remote Sensing and Spatial Information Sciences*, 36.

Brodu, N., and Lague, D. 2012. 3D Terrestrial Lidar Data Classification of Complex Natural Scenes Using a Multi-Scale Dimensionality Criterion: Applications in Geomorphology, *ISPRS Journal of Photogrammetry and Remote Sensing,* 68(1): 121-34.

CloudCompare. 2019. Computer Software – Version 2.10 Zephyrus. https://www.danielgm.net/cc/ [April 22, 2019]

Esri. 2019. Topographic and World Basemap. www.arcgis.com/home/item.html?id=30e5fe3149c34df1ba922e6f5bbf808f [April 19, 2019].

Fenton, M.M., Waters, E.J., Pawley, S.M., Atkinson, N., Utting, D.J., and Mckay, K. 2013. Surficial geology of Alberta; Alberta Energy Regulator, AER/AGS Map 601

Fey, C., and Volker, W. 2017. Long-Range Terrestrial Laser Scanning for Geomorphological Change Detection in Alpine Terrain – Handling Uncertainties. *Earth Surface Processes and Landforms,* 42: 789-802.

Golder and Associates. 1998. Geotechnical Investigation – November 1998 Report, *Geotechnical Risk Management Plan*.

Google Earth. 2015. Alberta, Canada. S. Alberta MD’s County – September 21, 2015. www.earth.google.com/ [April 19, 2019]

Government of Alberta. 2017. Alberta Highway 1 to 986 Traffic Volume History (2008 – 2017). www.open.alberta.ca/opendata/traffic-volumes-at-points-on-the-highway [April 25, 2019].

KCB. 2018. Geotechnical Drilling and Instrument Installation – February 2018 Report, *Geotechnical Risk Management Plan*.

Lague, D., Nicolas, B., and Jérôme, L. 2013. Accurate 3D Comparison of Complex Topography with Terrestrial Laser Scanner: Application to the Rangitikei Canyon (N-Z). *ISPRS Journal of Photogrammetry and Remote Sensing,* 82: 10-26.

Langley, R.B. 1998. RTK GPS, *GPS World*, 9(9): 70-76.

NRC. 2008. Canada’s Most Damaging Landslides. *Geofacts*. www.publications.gc.ca/collections/collection_2008/nrcan/M4-59-2-2008E.pdf [April 19, 2019].

Ophelia-Sensors. 2018. Product Information Page. www.ophelia-sensors.com/geocube [April 19, 2019].

Prior, G.J., Hathway, B., Glombick, P.M., Pana, D.I., Banks, C.J., Hay, D.C., Schneider, C.L., Grobe, M., Elgr, R., and Weiss, J.A. 2013. Bedrock geology of Alberta; Alberta Energy Regulator, AER/AGS Map 600

Rodriguez, J., Michael T.H., and Renato, M. 2018. Cost-Effective Landslide Monitoring GPS System: Characteristics, Implementation and Results, *Geohazards 7*, Canmore, Alberta, Canada.

Teledyne Optech. 2019. ILRIS-LR Specifications Sheet. info.teledyneoptech.com/acton/attachment/19958/f-02ea/1/-/-/-/-/ILRIS-LR-Spec-Sheet_LR.pdf [April 22, 2019]

Zhang, W., Qi, J., Wan, P., Wang, H., Xie, D., Wang, X., and Yan, G. 2016. An Easy-to-Use Airborne LiDAR Data Filtering Method Based on Cloth Simulation, *Remote Sensing,* 8(6):501.